Hardware-in-the-Loop Verification Environment for Heavy-Duty Hybrid Electric Vehicles

Ari Hentunen, Jussi Suomela, Antti Leivo, Matti Liukkonen and Panu Sainio
Aalto University School of Science and Technology, Espoo, Finland
Email: ari.hentunen@tkk.fi

***Abstract*—This paper presents an implementation of a versatile hardware-in-the-loop verification environment for heavy-duty hybrid electric vehicle (HEV) control software development. The verification environment is located at university facilities, and it consists of full-scale HEV systems that can be loaded with either an electric motor dynamometer or a programmable chassis dynamometer. Model-based software development tools and rapid control prototyping hardware are used to control the test bench hardware and to develop and execute control software. The verification environment can also be used e.g. to measure the efficiency of electric traction motors, power electronic converters, energy storages, and hydraulic pumps.**

I. Introduction

Due to tightening regulations for emissions and rising fuel prices, the original equipment manufacturers (OEMs) of mobile work machines have shown rising interest to hybridize the drivetrain. While in the automotive industry the focus is more on the cost issues, fuel economy, and emissions [1], [2], in the work machine industry the driving force in the hybridization is the desire to increase productivity and to decrease operating costs. Also safety and comfortability of the operator may be improved with e.g. more sophisticated diagnostics and ease of operation.

The desire to have less exhaust emissions and lower levels in the area of the noise-vibration and harshness (NVH) is obvious. In case of mobile work machines, internal combustion engine (ICE) output power based emission limits will strongly encourage the OEMs to downsize the engine as small as possible. Hybridization offers an excellent way to shift into a lower power class engine and at the same time keep up the productivity. Downsized engine offers lower exhaust emissions, less stringent regulations for emissions, and smaller auxiliary devices. Moreover, typically an electric drive offers pure rotational movements compared to the ICE's typical back-and-forth movement. In case of a hybrid electric vehicle (HEV), the possibility to use smaller ICEs with narrower area of operation gives also better tools to control the NVH matters. [3]

A system layout of a series hybrid electric vehicle (SHEV) is shown in Fig. 1. In SHEVs, all traction power is transferred in electrical form. The ICE acts only as a generator to provide electricity. Series hybrids are the most efficient in driving cycles that have repetitive starts and stops [4] and low averige and maximum speed. To achieve high efficiency, reasonably high voltage is usually used to decrease resistive losses. On the other hand, optimal battery voltage is usually lower than dc link voltage, and thus a dc–dc converter is often used between dc link and energy storage. The use of a dc–dc converter also allows more sophisticated power management strategies. Ultracapacitors (UCs) are good for duty cycles that include lots of acceleration and deceleration, or if the duty cycle includes very high power peaks that have short duration. In work machines, the engine may often be downsized drastically due to hybridization—even 50 %—because the engine of the conventional machine needs to be sized for the short-time peak power of the work cycle [5].

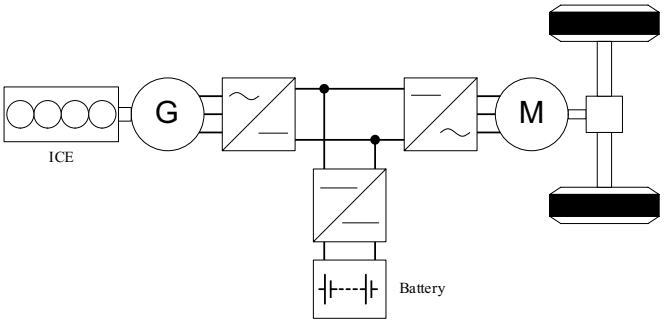

Fig. 1. Layout of SHEV.

HEVs have at least two energy sources. Usually the primary power source is either an ICE or a fuel cell (FC) stack, and peak power is provided with a battery or UC stack. Due to high price of FCs, ICE is the choice of most work machine OEMs. However, it is easy to replace the ICE with a FC system in future, because the ICE is only a source of electricity.

The advent of electric transmission into vehicles presents new challenges for vehicle manufacturers. Besides the selection of system topology and components, performance and fuel economy of a HEV depend strongly on the control strategy. OEMs need to develop new traction control algorithms as well as power management strategies to achieve design criteria. Furthermore, system integration and verification of software can be cumbersome, especially if the components have not been tested alone as well as together in a test environment that resembles the system under development.

Electrical power ratings of electric motors (EMs) and power electronic (PE) equipment for heavy-duty hybrids range from tens to hundreds of kilowatts, and response times of power electronic converters (PECs) are in the order of milliseconds. Since there are high currents and voltages as well as electric

978-1-4244-8218-4/10/$26.00 ©2010 IEEE

machines that are rotating with speeds up to 15 000 rpm in the system that is fully software controlled, special care should be taken in the development of control software. During early development it is also often necessary to update or even replace subsystems because of hardware problems. Thus, it is a good practice to develop control algorithms in a laboratory environment and—if possible—to use only verified algorithms in the prototype vehicle. [6], [7]

Model-based software development (MBSD) tools with rapid control prototyping (RCP) hardware are widely used in automotive industry as well as mobile work machine industry [8]–[16]. With these tools and hardware it is straightforward to develop control algorithms and to implement them using automatic code generation. Time consuming coding phase is not needed at all in early development and research.

In this paper, a full-scale hardware-in-the-loop (HIL) test environment is described in detail and its utilization possibilities are discussed and demonstrated with an example. Controller models and plant models are made with MATLAB/Simulink, and dSPACE RCP hardware is used as an electronic controller unit (ECU). As a case example, a simulation platform is first used to simulate the functionality of the control algorithms. Then, the plant models are validated in a HIL environment that consists of a dc power supply, UC stack, dc–dc converter, inverter, and EM. The load torque, which imitates the torque that is needed to accelerate or decelerate moment of inertia, is made with a dynamometer.

The paper is organized as follows. The HIL verification environment with full-scale hybrid system is described in section II. Controller models and plant models that are used in the simulations are described in section III. Experimental results of a HIL simulation and efficiency measurements are presented in section IV. Section V concludes the paper.

II. HIL VERIFICATION ENVIRONMENT

The system layout is shown in Fig. 2. The components are mostly off-the-shelf products that are available in the market. The nominal dc link voltage is 650 V, which is a common voltage rating for HEV buses and work machines [17].

There are two main switches (S_1 and S_2) in the system that connect the ac–dc converters to the mains, and a third switch S_3 that interconnects the dc link to the intermediate dc link of the frequency converter. All switches are to be switched only when the system is powered down. In this section, S_1 and S_2 are assumed to be closed and S_3 is assumed to be open. Hence, the dc buses are not connected together. The right-hand side from the switch S_3 is the HEV system under test (SUT). In the left-hand side there are an EM and a frequency controller, which comprise the dynamometer for the traction motor. The frequency converter incorporates a brake chopper, which is connected to a brake resistor to allow regenerative braking.

A. HEV system

The hybrid system has been configured to resemble a series-HEV topology. Hence, all HEV subsystems are connected to the common dc link. The HEV system consists of

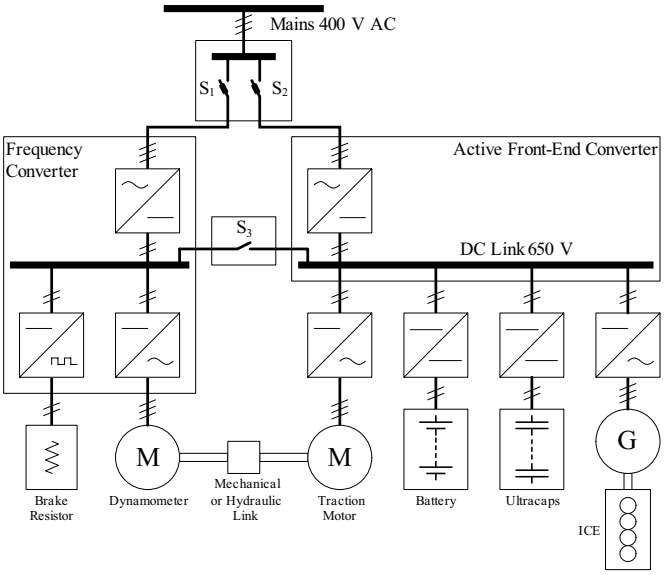

Fig. 2. Power hardware layout of the HIL verification environment.

- ICE–generator set (gen-set) with a generator inverter
- ultracapacitor module with a bidirectional dc–dc converter
- battery with a bidirectional dc–dc converter
- traction motor and inverter

The system also includes a dc power supply that can be used to provide dc power if the gen-set and battery are used in the test setup. The dc power supply takes power from the mains and regulates the dc link voltage to the desired value, usually 650 V. If the power coming to the dc link is balanced with the power that is taken from the dc link, then no power is taken from the mains. Otherwise, power from the mains equals the difference of consumed and generated average power in the dc link. Thus, the dc supply actually acts like a battery in the dc link.

1) Gen-set unit: The diesel engine is AGCO Sisu Power 49 DTAG, which has continous power rating 92 kW at 1 500 rpm, and limited time power rating 102 kW at 1 500 rpm [18]. The engine speed can be controlled via controller area network (CAN) bus. It is possible to choose from five pre-defined torque–speed curves, and in addition to that, torque can be limited with a CAN message. Hence, it is possible to provide any torque–speed characteristics below the original curves by having a look-up table in the control software and adjusting the torque limit with the operating point. However, in that case, the engine characteristics such as fuel consumption and emissions do not resemble any real engine characteristics anymore, and e.g. fuel consumption may be poor compared to a real engine, because the engine characteristics are optimized in a different operating point.

The original generator of the SG 115 diesel-generator system has been replaced with a permanent magnet axial-flux generator, which is manufactured by AXCO-Motors [19]. The generator has eight poles and its power rating is 120 kVA at

2 000 rpm. The generator is directly coupled to the crankshaft of the engine. The generator is developed for HEVs and is liquid-cooled.

Together the diesel engine and the generator constitute a variable-speed diesel-generator (VSDG) set that has a maximum speed of 2 000 rpm, maximum power of 120 kVA, and maximum electrical angular frequency of 133 rad/s. The ac from the generator is then converted to regulated dc voltage with a frequency converter that is operating in dc link voltage control mode. The input ac is not connected, but the dc link of the frequency converter is connected to the common dc link. The manufacturer of the frequency converter is ABB and the type code of the converter is ACSM1-04LS-260A-4+K457 [20]. The converter is liquid cooled, and it is controlled via CAN bus. The continuous power is 160 kW. The converter incorporates also a brake chopper, and a brake resistor will be installed in it.

2) Electric traction drive: The traction motor and inverter are manufactured by Siemens and are from the electric drive system ELFA [17]. The components are made for electric drivetrain applications, and thus are liquid-cooled. ELFA includes also an ECU that is called DICO, which has upper level control software for controlling a complete hybrid system. However, that functionality has been disabled, and thus, DICO acts merely as a gateway between CAN bus and DCAN bus, which ELFA uses in the inner communication between subsystems.

The motor type is 1PV5135-4WS28. It is an induction machine with four poles. The nominal torque is 160 Nm and power 67 kW at 4 000 rpm, respectively. The maximum torque is 430 Nm and power 150 kW at 2 500 rpm, respectively. Maximum speed is 10 000 rpm.

The inverter type is G650 D440/170/170 M7-1. The inverter actually includes two three-phase insulated gate bipolar transistor (IGBT) inverters and two brake choppers. However, only one inverter is in use in the test system. Nominal input voltage is 650 V dc. Rated output voltage is 440 V ac, continuous current 170 A, and maximum current 300 A, respectively.

3) Ultracapacitor: A BMOD0018 P390 (HTM power series 390v) from Maxwell Technologies is used as an ultracapacitor module. The capacitance of the module is 17.8 F and the nominal voltage is 390 V. The module consists of 146 series connected 2.7 V cells, and its nominal current is 150 A and maximum current 950 A. HTM power series 390v is not in production anymore.

4) Battery: Lithium-polymer battery consists of 98 cell that are connected in series. Battery manufacturer is Kokam, and the cell type is SLPB 100216216H, which is a 40 Ah cell [21]. The nominal voltage is 3.7 V, minimum voltage 2.7 V, and maximum voltage 4.2 V, respectively. Maximum charge current is 80 A, nominal discharge current 200 A, and maximum discharge current for 10 s is 400 A, respectively.

Battery cells are pre-assembled in modules that have seven cells connected in series and include voltage measurements for each cell and four temperature measurements, which are located between every other two adjacent cells. A variable-speed cooling fan has been added in front panel of each module, and vent holes have been made in sides of the modules. The battery comprises 14 modules that are connected in series. The nominal voltage of a module is 25.9 V, and thus, the nominal voltage of the battery is 362 V. One extra battery module is also available in the laboratory to be tested separately.

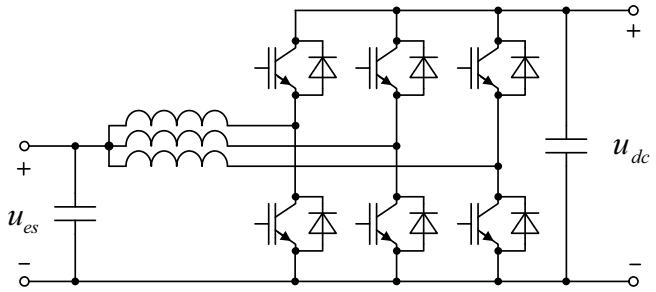

Fig. 3. Bidirectional three-phase boost converter.

The battery management system (BMS) is manufactured by Elithion [22]. It consists of a BMS controller and 14 cell boards, one for each battery module. Cell boards are located inside battery modules. The extra battery module has its own BMS.

5) DC–DC converter: The bidirectional three-phase boost converter topology is shown in Fig. 3. The converter is manufactured by MSc Electronics [23] and its model is 200DCDC750A2SN. The converter utilizes multi-phase interleaving, which reduces current ripple. The nominal ES side current of the converter is 120 A and the maximum current is 200 A.

The converter is controlled with a current reference. Also hardwired tunable minimum and maximum voltage limits for the input and the output are incorporated into the control system to prevent over- and undervoltages in the system. The voltage of the energy storage (ES) needs to be lower than the dc link voltage. If the dc link voltage decreases and goes below the ES voltage, the diodes in the power stage begin to conduct current from the ES to the dc link, and thus, the voltages stay equal until the dc link voltage starts to rise. The minimum current of the converter is 20 A.

6) DC power supply: Vacon Active Front-End (AFE) with NXA_0460 5 input module [24] is used as a dc power supply. The nominal ac current is 460 A and the continuous dc output power rating is 310 kW. AFE includes a three-phase IGBT bridge, an LCL line filter, and a pre-charge circuit. AFE regulates the dc link voltage the desired setpoint. The recommended output voltage range is about 600–700 V dc for 400 V ac mains voltage. The input power factor can be set to unity, thus no reactive power is consumed.

AFE can be controlled and monitored via CAN bus or from the panel. It is possible to set a positive and a negative current limit. However, if the consumed power is more than the current limit allows, the dc link voltage decreases, and at a certain point, the diodes of the IGBT bridge begin to conduct and keep the dc link voltage at rectified mains voltage of 540 V.

7) Mechanics: The mechanical environment is built on high insulation rubber floor using T-slot beams with weight of 500 kg each. Also all fastening components have been overdimensioned by purpose to have a very rigid mounting and to avoid the need for unnecessary flexible couplings. The couplings used are jaw-type couplings, thus allowing axial plug-in, good dynamics, vibration reduction, and failsafe behavior. In case of overload, they do allow some torsional flexibility.

B. Load dynamometer

An electric motor dynamometer is used to load the traction motor. The motor manufacturer and model are the same as the traction motor, which is attached to the test bench (subsection II-A2). However, the original speed sensor has been replaced with SICK CKS36 Encoder, which has resolution of 1 024 bit/rev.The dynamometer can be used to test also other traction motors by replacing the equipment under test (EUT) with another EM.

Vacon NXP frequency converter with an inverter unit INU_0300 5 is used to control the EM. Frequency converter can be controlled and monitored via CAN bus. The motor can be controlled either with a torque reference with a speed limit or with a speed reference with a torque limit.

When the dynamometer is braking the traction motor, and hence, acting as a generator, the braking power is dumped to the brake resistor through the brake chopper. The dc links of the frequency converter and AFE can also be interconnected by closing the switch S_3. Then, the generated power flows back to the dc link and can be used e.g. to provide power to the traction motor. If the tractive power is provided by the gen-set or battery, then AFE feeds the generated power back to the mains.

C. Measurement equipment

Torque and speed are measured with a KTR Dataflex 42/1000 transducer.

Norma D6100 power analyzer has been used to measure power and efficiency of the EUT. Measurement data were transferred through RS232 link to the host computer.

A new Hioki 3390 power analyzer with a motor testing and D/A output option has been acquired to the laboratory. Currents are sensed with ac/dc clamp on CT 9278 current clamps, which have a maximum continuous input current of 350 A for a bandwidth of 19 kHz, 200 A for 40 kHz, and 100 A for 100 kHz, respectively.

Ultracapacitor voltage is measured with LEM AV100-750 transducer and current with LEM LA 305-S transducer, respectively.

D. Other equipment

In the laboratory facilities, also a programmable chassis dynamometer for two wheels and a cold/warm chamber that has a temperature range of $-50 \ldots +50\,^{\circ}\mathrm{C}$ are available. The size of the chamber is big enough to drive a van inside.

E. Cooling circuit

A common rail liquid cooling circuit with six independent branches that are controlled with electrically operated valves is used to provide proper cooling for liquid-cooled subsystems. An electric pump from EMP is used to control the flow in the common rail, and electrical valves are used to open and close branches. Flow, pressure, and temperature data from each branch are measured and sent to the ECU.

From the cold chamber circulation there is available separate -20 C circulation of water-glycol mixture, if extensive cooling circulation is needed.

F. Control system

Almost all laboratory equipment is controlled with a dSPACE MicroAutoBox (MABX) DS1401/1505/1507 RCP ECU. It has four CAN buses and lot's of analog and digital I/O. The voltage level of the digital I/O is 5 V, analog inputs 5 V, and analog outputs 4.5 V, respectively. However, because voltage levels of some devices is exceed those, some additional analog and digital I/O has been implemented using Beckhoff's industrial automation I/O modules. Beckhoff's I/O modules communicate with MABX via CAN bus.

MBSD is utilized to produce code for the RCP ECU. Models are made with MATLAB/Simulink/Stateflow. Also Real-Time Workshop and dSPACE RTI blockset are needed to generate C code from the Simulink model. The compiled code is then uploaded into the MABX, after which the controller starts executing the real-time program. The ECU is connected to the host computer via high speed link. All measurements as well as other signals can be monitored online from the host computer through dSPACE ControlDesk. A graphical user interface (GUI) has been made for every device that is controlled with the ECU. It is also possible to tune online e.g. the constant parameters and the gains of the original model. This makes it easy to implement manual controls of the laboratory equipment directly from the host computer.

III. Simulation models

A. Simulation platform

A flexible simulation platform has been created that includes a library of easily parametrizable plant models of HEV systems, e.g. electric motors, inverters, dc–dc converters, battery, ultracaps, gears, ICE, etc. With the simulation platform, it is easy to simulate different kind of hybrid work machines and to develop control strategies for them. Simulation time-step is 1 ms. Backward functional modeling from the imposed load cycle is utilized in simulating the HEV system. The load cycle can be a mechanical load for EMs or an electrical load that is formed e.g. from the measured traction power data of a conventional machine.

The accuracy of the models has been defined to resemble large signal behavior and to neglect very fast transients and all switching frequency characteristics of PE converters. This is because simulated driving cycles are long, e.g. 60 s, and on the other hand, detailed models that include switching behavior take very long time to execute. Furthermore, very detailed

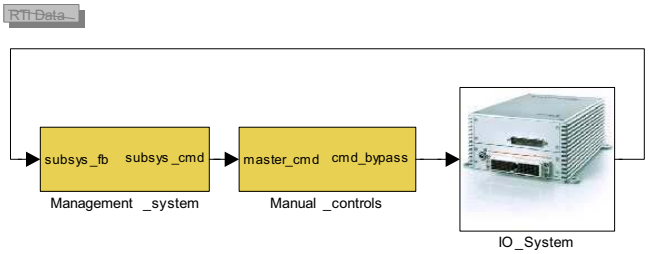

Fig. 4. Top level of the controller model.

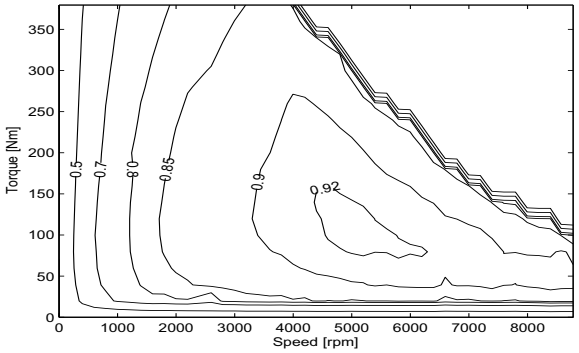

Fig. 5. Combined measured efficiency map of Siemens ELFA 1PV5135-4WS28 traction motor and G650 D440/170/170 M7-1 inverter.

information of the devices' components and controllers should be known to model the exact behavior.

In order to achieve good accuracy for the fuel consumption, and to be able to develop control algorithms that work also in real life, detailed information about the efficiency of the devices in the hybrid drive train is needed. Unfortunately, such information is rarely available from the subsystem suppliers. Manufacturers often give the efficiency information only in the nominal point. However, in order to find out real efficiencies in whole operation range, efficiency map measurements have been done for the devices of the HIL verification environment, and the measured efficiency maps are used in the simulation models.

B. Controller models

The top level of the controller model that runs in MABX is shown in Fig. 4. The main model has two parts, the management system and the I/O system. In addition, the manual controls submodel is placed between the two. Management system submodel is the real vehicle control software that has all the control algorithms running. However, it is possible to bypass the control outputs of the management system with manual controls by selecting manual control mode in the manual controls subsystem for individual devices. ControlDesk can be used to give control inputs for manually controlled devices as well as for the management system.

The implementation of the I/O is carried in the I/O system submodel. It includes e.g. signal routing, signal scalings, and target-specific blocks from dSPACE I/O library.

IV. Experimental results

A. Efficiency measurements

Norma D6100 power analyzer was used to measure the efficiency maps of the traction motor, inverter, dc–dc converter, and ultracapacitor module. During efficiency measurements of the traction motor and inverter, the switch S_3 from Fig. 2 was set to closed-position and S_1 to open-position, respectively. This allows the braking power of the dynamometer to be used to provide power for the traction motor. Thus, only losses are taken from the mains.

The efficiency map measurement of the traction motor and inverter were done by controlling the dynamometer with a speed reference and the EUT with a torque reference, respectively. The speed range was measured at speed intervals of 200 rpm. In each speed setpoint, torque range was measured at torque intervals of 20 Nm. The measurements were made after a steady-state had been achieved. Norma D6100 power analyzer was used in this measurement. The power analyzer can calculate electrical power of a three-phase symmetrical load from measurements of two phase currents and two line-to-line voltages. Torque and speed data were collected from the respective transducers to calculate mechanical power. Inverter's input power and output power were measured. The efficiency maps of the motor and inverter were both measured, but in the simulation model it is enough to have a combined efficiency map that includes both the inverter and the motor. The measured combined efficiency map is shown in Fig. 5. It can be seen that best efficiency can be achieved with speeds beyond the nominal point of the motor.

B. HIL simulation of SHEV load sharing algorithm

Simulation model validation is demonstrated with a HIL simulation, where an UC stack is used to provide peak power during short power peaks. Thus, the primary power source—e.g. an ICE or a fuel cell—dynamics need not be as fast, and the primary power source can be downsized. In this HIL simulation, the dc power supply was used to emulate the primary power source. The load power was made with the EM dynamometer. The control stategy, plant models, and experimental results are described in more detail in [25].

Two modeling principles for the ultracapacitor were used in the simulation: constant capacitance (constant C) with equivalent series resistance (ESR), and variable capacitance (variable C) with ESR. In the constant C model, the nominal capacitance value was used. In the variable C model, the capacitance has been calculated from the constant current measurements, and a capacitance mapping has been defined based on the calculations, i.e. the capacitance depends on the voltage and current.

Validation measurements are shown in Figs. 6 and 7. It can be seen that the simulated and measured currents and voltages match quite well. However, there are some abnormalilities especially in the currents. These are due to several reasons, one being the dc–dc converter's minimum current of 20 A,

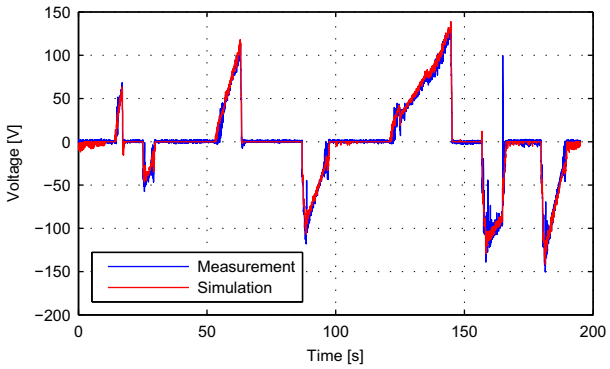

Fig. 6. Comparison of measured and simulated dc–dc converter current.

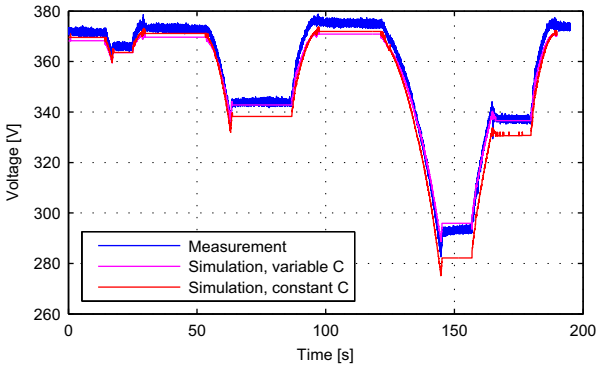

Fig. 7. Comparison of measured and simulated ultracapacitor voltage.

which causes differences in near zero current, even though that functionality is modeled in the plant model. Another cause for differences is that the exact behavior of the dc power supply's voltage regulator is hard to model. However, the mean error is only -0.32 A and the rms error 5.7 A. For the UC voltages, the variable C model gives more accurate results with mean error of 1.7 V and rms error 3.0 V.

V. Conclusion

A versatile HIL verification environment for HIL simulations of heavy-duty hybrids with full-scale hybrid electric power system was presented. The system is located at university facilities and it can be used for research and education purposes as well as for making case-study HIL simulations for work machine manufacturers. This test facility has been used e.g. to measure the efficiencies of PECs, EMs, and hydraulic pumps, to characterize devices and validate plant models, to make experimental HIL simulations to verify and validate HEV control algorithms, to provide load cycles for energy storage testing, and to provide high and controllable electric power for various other research equipment.

Acknowledgment

This study has been carried in HybDrive and HybLab projects funded by the Finnish Funding Agency for Technology and Innovations (Tekes) and Multidisciplinary Institute of Digitalization and Energy (MIDE) of Aalto University School of Science and Technology, respectively.

References

[1] C. C. Chan, "The state of the art of electric, hybrid, and fuel cell vehicles," *Proc. IEEE*, vol. 95, no. 4, pp. 704–718, 2007.
[2] A. Emadi, Ed., *Handbook of Automotive Power Electronics and Motor Drives*. Boca Raton, FL: CRC Press, 2005.
[3] *World Heavy Construction Equipment to 2009*, Industry study number 1964, The Freedonia Group, Cleveland, OH, 2005.
[4] O. D. Momoh and M. O. Omoigui, "An overview of hybrid electric vehicle technology," in *Proc. IEEE Vehicle Power and Propulsion Conference*, Dearborn, MI, Sep. 2009, pp. 1286–1292.
[5] T. Lehmuspelto, M. Heiska, A. Leivo, and A. Hentunen, "Hybridization of a mobile work machine," *World Electric Vehicle Journal*, vol. 3, 2009. [Online]. Available: http://www.evs24.org/wevajournal/
[6] M. J. Marcel, T. A. Haskew, and K. A. Williams, "Test facility for a hybrid fuel cell electric vehicle," *Proc. IEEE*, pp. 734–739, Mar. 2007.
[7] R. M. Schupbach and J. C. Balda, "A versatile laboratory test bench for developing powertrains of electric vehicles," in *Proc. IEEE Vehicular Technology Conference 2002 Fall*, vol. 3, Vancouver, Canada, Sep. 2002, pp. 1666–1670.
[8] J. Weber, *Automotive Development Processes: Processes for Succesful Customer Oriented Vehicle Development*. Berlin, Germany: Springer, 2009.
[9] S. C. Nagaraj and B. Detrick, "HIL and RCP tools for embedded controller development in hybrid vehicles," in *Proc. IEEE Vehicle Power and Propulsion Conference*, Dearborn, MI, Sep. 2009, pp. 896–902.
[10] A. Wagener, P. Seger, C. Koerner, and H. Kabza, "Simulation-based automatic code-generation for ECUs in distributed control systems, applied in a testbed for a hybrid vehicle drivetrain," in *Proc. IEEE International Symposium on Industrial Electronics*, vol. 2, Cholula, Puebla, Mexico, Dec. 2000, pp. 643–648.
[11] A. Leivo, J. Suomela, and A. Hentunen, "Model reusability and co-operation in model based HEV control system development," in *Proc. Electric Vehicle Symposium (EVS 24)*, Stavanger, Norway, May 2009.
[12] C. Lin and L. Zhang, "Hardware-in-the-loop simulations and its application in electric vehicle development," in *Proc. IEEE Vehicle Power and Propulsion Conference*, Harbin, China, Nov. 2008.
[13] H. Hu, G. Xu, and Y. Zhu, "Hardware-in-the-loop simulation of electric vehicle powertrain system," in *Proc. Power and Energy Engineering Conference*, Wuhan, China, Mar. 2009.
[14] A. Bouscayrol, W. Lhomme, P. Delarue, B. Lemaire-Semail, and S. Aksas, "Hardware-in-the-loop simulation of electric vehicle traction systems using energetic macroscopic representation," in *Proc. IEEE 32nd Annual Conference on Industrial Electronics (IECON 2006)*, Paris, France, Nov. 2006, pp. 5319–5324.
[15] A. Bouscayrol, "Different types of hardware-in-the-loop simulation for electric drives," in *Proc. IEEE International Symposium on Industrial Electronics (ISIE 2008)*, Cambridge, UK, Jun. 2008, pp. 2146–2151.
[16] Y. Cheng, J. V. Mierlo, P. Lataire, and G. Maggetto, "Test bench of hybrid electric vehicle with the super capacitor based energy storage," in *Proc. IEEE International Symposium on Industrial Electronics (ISIE 2007)*, Vigo, Spain, Nov. 2007, pp. 147–152.
[17] Siemens electric drive system ELFA. [Online]. Available: http://www.siemens.com/elfa/
[18] AGCO Sisu Power homepage. [Online]. Available: http://www.agcosisupower.com/
[19] AXCO-Motors homepage. [Online]. Available: http://www.axcomotors.com/
[20] ABB homepage. [Online]. Available: http://www.abb.com/
[21] Kokam homepage. [Online]. Available: http://www.kokam.com/
[22] Elithion homepage. [Online]. Available: http://www.elithion.com/
[23] MSc Electronics homepage. [Online]. Available: http://www.mscelectronics.fi/
[24] Vacon homepage. [Online]. Available: http://www.vacon.com/
[25] M. Liukkonen, A. Hentunen, and J. Suomela, "Validation of quasi-static series hybrid electric vehicle model," in *Proc. IEEE Vehicle Power and Propulsion Conference*, Lille, France, Sep. 2010. (in press).